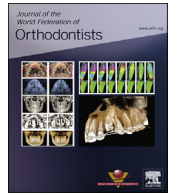


Contents lists available at [ScienceDirect](https://www.sciencedirect.com)

## Journal of the World Federation of Orthodontists

journal homepage: [www.jwfo.org](http://www.jwfo.org)

## Research Article

## Evaluation of stress pattern in periodontium and change in inclination during en masse retraction: Finite element analysis

Himanshu Kalia<sup>a</sup>, Seema Gupta<sup>b</sup>, Sachin Ahuja<sup>c,\*</sup>, Eenal Bhambri<sup>d</sup>, Ankit Goyal<sup>a</sup>, Rohini Sharma<sup>e</sup><sup>a</sup> Postgraduate student, Department of Orthodontics and Dentofacial Orthopedics, Surendera Dental College and Research Institute, Sriganaganagar, Rajasthan, India<sup>b</sup> Professor, Department of Orthodontics and Dentofacial Orthopedics, Surendera Dental College and Research Institute, Sriganaganagar, Rajasthan, India<sup>c</sup> Professor and Head, Department of Orthodontics and Dentofacial Orthopedics, Surendera Dental College and Research Institute, Sriganaganagar, Rajasthan, India<sup>d</sup> Reader, Department of Orthodontics and Dentofacial Orthopedics, Surendera Dental College and Research Institute, Sriganaganagar, Rajasthan, India<sup>e</sup> Senior Lecturer, Department of Orthodontics and Dentofacial Orthopedics, Swami Devidayal Hospital and Dental College, Barwala, Panchkula, Haryana, India

## ARTICLE INFO

## Article history:

Received 29 April 2019

Accepted 8 July 2019

Available online 16 August 2019

## Keywords:

Anterior retraction hook

Center of resistance

FEM

Mini-implants

## ABSTRACT

**Objective:** Understanding the effects of retraction accompanied by intrusion on the periodontium of the anterior teeth along with the change in displacement during the en masse retraction of the maxillary anteriors using orthodontic mini-implants (OMIs) and retraction hooks at different levels.

**Design:** Finite element analysis.

**Materials and method:** The finite element model of maxillary dentition was made using a computed tomographic scan. The implants of 1.5 × 8.0-mm dimensions were inserted at an angle of 90° at distance of 7 mm (low OMI) and 10 mm (high OMI) with anterior retraction hooks (ARH) at 3, 6, and 9 mm. Six models were constructed for the study. After the boundary conditions were defined, 200 g of retractive force was applied from ARH at low and high OMI traction. The stresses on periodontal ligament (PDL), bone, bone surrounding implant, and cementum, along with change in inclination and displacements of anterior and posterior teeth along the y- and z-axis were determined.

**Results:** An overall tipping and extrusion was seen in all the cases. Low OMI placement with retraction hooks at 3 mm and 6 mm showed more tipping movements, whereas high OMI with 9-mm ARH showed more bodily movement. Both high and low OMI with 9-mm ARH showed more root movement. The stresses in PDL, bone, and cementum were less at 3-mm ARH in both low and high OMI groups. The stresses were more in cortical bone than cancellous bone and also more on lateral incisors than central incisors.

**Conclusion:** If controlled lingual tipping of anterior teeth is required with minimum torque loss, high OMI with low ARH is recommended, whereas if lingual root movements with retraction is required, high OMI and high ARH is recommended.

© 2019 Published by Elsevier Inc. on behalf of World Federation of Orthodontists.

## 1. Introduction

Extraction is the most common way of gaining space in orthodontics. During the space closure when forces are applied, there are favorable as well as unfavorable movements. The responses of these forces on the tooth and the moments must, therefore, be studied so as to reduce empiricism in the orthodontic treatment. Anchorage has been a significant consideration for orthodontists and is one of the important components in treatment planning. Orthodontic mini-implants (OMIs) have modernized the concept of orthodontic anchorage by making anchorage perfectly balanced [1].

During the movement of the anterior teeth, stresses are generated in the periodontium. These stresses must be considered while

Funding: The authors have not declared a specific grant for this research from any funding agency in the public, commercial or not-for-profit sectors.

Competing interest: Authors have completed and submitted the ICMJE Form for Disclosure of potential conflicts of interest. None declared.

Patient/Parent consent: Authors have obtained and submitted the patient signed consent form.

Provenance and peer review: Not commissioned; Externally peer reviewed.

\* Corresponding author: Professor and Head, Department of Orthodontics and Dentofacial Orthopedics, Surendera Dental College and Research Institute, Sriganaganagar, Rajasthan, India 335001.

E-mail address: [drsachinahuja@hotmail.com](mailto:drsachinahuja@hotmail.com) (S. Ahuja).

**Table 1**  
Material characteristics used in the study

Material	Young's modulus (GPa)	Poisson's ratio ( $\nu$ )
Enamel	77.9	0.33
Dentin	16.6	0.31
Cementum	15	0.31
PDL	0.05	0.45
Cortical bone	10	0.26
Cancellous bone	0.5	0.38
Titanium	105	0.37
NiTi	80	0.33

NiTi, nickel titanium; PDL, periodontal ligament.

planning treatment. Unbalanced forces may lead to unwanted stresses, which may lead to root resorption [2]. Thus, evaluation of stresses during various combinations of force application must be studied to understand the nature of stress and the sites of maximum and minimum stress during these movements. One of the methods to study the stresses is finite element analysis (FEM) [3], which provides the orthodontist with quantitative data that can extend the understanding of the physiologic responses of the dentition to orthodontic forces.

Many studies have evaluated the change in displacement of anterior teeth in mini-implant–assisted retraction [4,5]. However, there are limited studies that evaluated the stresses on the bone (around the teeth and implants), cementum, and periodontal ligament (PDL) during en masse retraction of the anterior teeth [6]. Therefore, the aim of the present study was to evaluate the biomechanical effects of retraction forces on periodontium during en masse retraction of anterior teeth with various combinations of OMI and retraction hooks (ARH) to identify a better combination of the previously mentioned factors.

## 2. Material and method

### 2.1. Generating of 3D geometric model

Computed tomography CT scan data of the skull was processed using MIMICS 8.1 software (Materialise NV, Leuven, Belgium), DICOM images were selected and converted into STL format, only region of interest (maxilla in this study) was selected [7].

### 2.2. Conversion of three-dimensional geometric model into finite model

Conversion was done by using Hypermesh version 13.0 (Hypermesh, MMr. Rupees, Bangalore, India). The model of maxillary dentition with bilateral first premolar extraction was simulated (HyperWorks CAE Software, Altair Engineering, MI). Each tooth was divided into enamel, dentin, and cementum, whereas the bone was divided into cortical and cancellous bone. The PDL was kept consistently at a thickness of 0.2 mm. The Young's modulus and Poisson's ratio for the structures and components used in the study

were set according to the finite element studies conducted previously, as shown in Table 1.

Using ANSYS software version 12.1, 0.022 × 0.028-inch MBT brackets and molar tubes, with the specific tip and torque values were modeled and placed according to MBT prescription (SIEMENS, DICOM, Syngo CT 2006 C2 format). The interface between the teeth and the bracket was connected, to avoid the interference of the composite bonding material. At the interfacial nodes between the archwire and the brackets, only sliding without friction was allowed to prevent unnecessary bracket-wire interplay. Six three-dimensional models were designed for the study as follows:

Model 1: ARH of 3 mm with low OMI of 7 mm (Fig. 1A)

Model 2: ARH of 6 mm with low OMI of 7 mm (Fig. 1B)

Model 3: ARH of 9 mm with low OMI of 7 mm (Fig. 1C)

Model 4: ARH of 3 mm with high OMI of 10 mm (Fig. 2A)

Model 5: ARH of 6 mm with high OMI of 10 mm (Fig. 2B)

Model 6: ARH of 9 mm with high OMI of 10 mm (Fig. 2C)

Arch wire of 0.019 × 0.025-inch stainless steel (SS) with ARH of 0.05-inch SS at varying heights between the canine and lateral incisor brackets were placed on a three-dimensional model. The mini-implants of dimensions 1.5 mm × 8 mm and 90° to the occlusal plane [8] were placed between the roots of the second premolars and first molars at varying heights from the arch wire. The force of 200 g simulating sliding mechanics was applied from heights of OMI to each ARH.

### 2.3. Defining the boundary conditions

After completion of the model fabrication, the boundary conditions were assigned at all peripheral nodes of bone with 0 degree of movement in all direction.

### 2.4. Interpretation of results

For baseline coordination system, the displacement of nodes along y-axis signified tooth movement in labio-palatal plane for incisors and mesio-distal plane for canine and posteriors, whereas z-axis denoted superior-inferior movements along the vertical plane. After applying the boundary conditions, the results were analyzed. von Mises stresses at PDL, cementum, bone, implant, and bone surrounding the implant were evaluated along with the principal stresses at PDL and cementum. The change in inclination was also assessed by the nodal displacement of the incisal edge and root apex. The initial displacement of the teeth was analyzed in the y- and z-axis.

## 3. Results

### 3.1. Stress distribution in bone

In all the models, the maximum von Mises stresses were seen at the disto-cervical region of the canines. These stresses reduced as

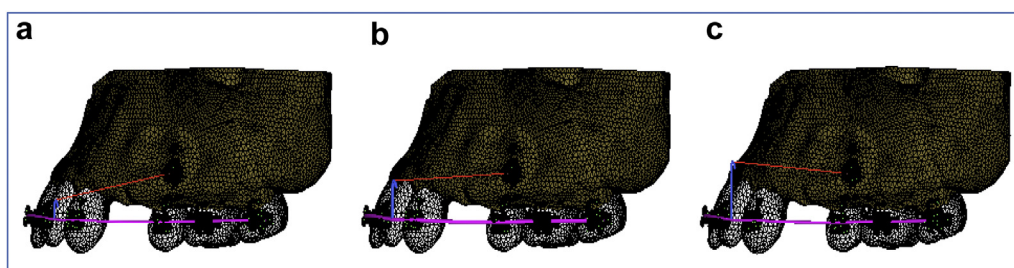


**Fig. 1.** (A) Model 1 with implant at 7 mm with retraction hooks at 3 mm. (B) Model 2 with implant at 7 mm with retraction hooks at 6 mm. (C) Model 3 with implant at 7 mm with retraction hooks at 9 mm.

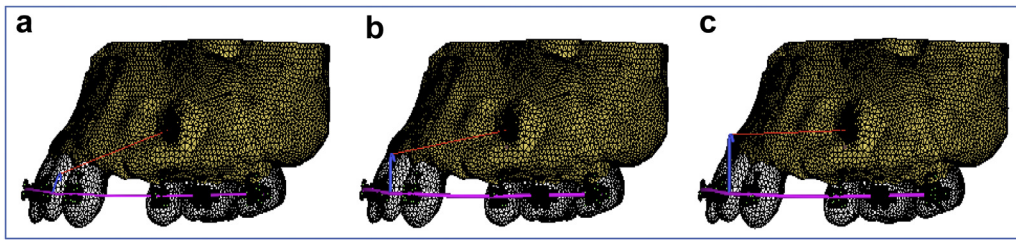


**Fig. 2.** (A) Model 4 with implant at 10 mm with retraction hooks at 3 mm. (B) Model 5 with implant at 10 mm with retraction hooks at 6 mm. (C) Model 6 with implant at 10 mm with retraction hooks at 9 mm.

the height of the retraction hook increased in cortical bone, whereas the opposite was seen in the cancellous bone. The maximum von Mises stress in the cortical bone was seen in model 1 (33.2 MPa) with the least in model 6, whereas in the cancellous bone, the maximum von Mises stresses were seen in model 3 and the least in model 4 (Table 2).

### 3.2. Stress distribution in bone surrounding implant

In all the models, the maximum von Mises were seen in the bone surrounding the implant. The maximum stresses were seen in the mesial area of the bone in the area of implant insertion and the stresses decreased with the increase in the height of the retraction hook for all the models. The maximum von Mises stress of 63.2 Mpa was seen in the mesial area of bone adjacent to implant insertion in Model 1, whereas the least stresses were seen in Model 6 (Table 2). The stresses in the cortical bone were more compared with cancellous bone in all the models.

### 3.3. Stress distribution in PDL

In all the models, the maximum von Mises stresses in PDL were seen at the apical area of the tooth and the maximum principal stresses were also present at the apical region with the compressive stresses at the lingo-cervical area of the root and the tensile stresses at the labio-apical area for all the anterior teeth. In the first molar, the maximum von Mises were at the apical area of the mesio-buccal (MB) root. The compressive stresses were present at the mesial aspect of the MB root (toward the furcation area), whereas the tensile stresses were seen at the buccal and distal aspects of the MB root (Table 3).

### 3.4. Stress distribution in cementum

In all the models, the maximum von Mises were seen at the cervical area of the anterior teeth. The compressive stresses were seen at the mid-root and apical area and the tensile stresses were noticed at the labio-cervical area of the root for all the incisors. In the canines, the distal side had compressive stress and the mesial side had tensile stress. In the MB root of first molar, the maximum von Mises and principal stresses were present at the cervical area. Because the MB root showed mesial tipping, the compressive stresses were seen at the mesial aspect near the cervical area, whereas the tensile stresses were seen at the buccal aspect of the cervical area (Table 4).

### 3.5. Displacement of teeth along y- and z-axis

The displacement in all the models for the anterior teeth and MB root of first molar along the y-axis and z-axis is depicted in Table 5. On evaluation of movement of teeth in the y- and z-axis, the following were seen:

#### 3.5.1. Central incisors

In both low and high OMI models, lingual tipping was seen with more crown movement, except in model 6 where more of bodily type movement was noticed. They also displayed extrusion in all models. The amount of extrusion was less in high OMI than low OMI and less amount of extrusion of root as compared with crown.

#### 3.5.2. Lateral incisors

The tipping was less as compared with centrals in the low OMI group, whereas in the high OMI group they displayed bodily type tooth movement at 3- and 6-mm ARH. At 9-mm ARH, more of palatal movement of root was seen as compared with crown in both low and high OMI groups. The laterals were less extruded as compared with centrals in low OMI cases. There was almost the same amount of extrusion of crown and root at 3- and 6-mm ARH and at 9-mm ARH, more root extrusion was seen compared with crown.

#### 3.5.3. Canines

Canines displayed distal tipping in all models, with more crown movement compared with root. They also showed extrusion in all models, which was more than incisors and the amount increased with increase in the height of ARH.

#### 3.5.4. MB root of first molar

The distal tipping of the MB cusp was noticed in models 1, 2, 3 and 4, whereas in models 5 and 6, both crown and root moved distally. Slight extrusion was seen in molars at MB cusp in all the models.

### 3.6. Change in inclination of anterior teeth

On analyzing the amount of torque loss, it was noticed that 3-mm ARH with high OMI had minimum amount of torque loss and displayed controlled movements compared with other combinations. The laterals displayed less amount of torque loss as compared with the centrals, as they were close to the point of force application and center of resistance (CR) of anterior teeth (Table 6).

## 4. Discussion

Different malocclusions require different treatment modalities. Extraction is the most common option for space gaining in

**Table 2**  
von Mises stresses in bone (MPa)

Reference point	Low OMI (7 mm)			High OMI (10 mm)		
	3 mm	6 mm	9 mm	3 mm	6 mm	9 mm
<b>Bone</b>						
Cortical bone	33.2	30.63	29.6	30.76	28.23	25.21
Cancellous bone	1.3	1.46	1.65	1.2	1.34	1.35
<b>Bone surrounding implant</b>						
Cortical cone	63.2	58.5	51.9	60.09	51.37	41.16
Cancellous bone	2.77	2.69	2.44	2.26	2.03	1.87

OMI, orthodontic mini-implants.

**Table 3**  
von Mises and principal stresses in PDL (MPa)

Tooth	Stress	Low OMI (7 mm)			High OMI (10 mm)		
		3 mm	6 mm	9 mm	3 mm	6 mm	9 mm
CI	von Mises	$8.9 \times 10^{-4}$	$1.04 \times 10^{-3}$	$1.08 \times 10^{-3}$	$8 \times 10^{-4}$	$9.5 \times 10^{-4}$	$1.01 \times 10^{-3}$
	Tensile	$4.1 \times 10^{-3}$	$5.15 \times 10^{-3}$	$5.51 \times 10^{-3}$	$3.4 \times 10^{-3}$	$4.5 \times 10^{-3}$	$5.01 \times 10^{-3}$
	Compressive	$-4.03 \times 10^{-3}$	$-4.62 \times 10^{-3}$	$-4.73 \times 10^{-3}$	$-3.6 \times 10^{-3}$	$-4.2 \times 10^{-3}$	$-5.46 \times 10^{-3}$
LI	von Mises	$1.2 \times 10^{-3}$	$1.49 \times 10^{-3}$	$1.58 \times 10^{-3}$	$1.1 \times 10^{-3}$	$1.4 \times 10^{-3}$	$1.5 \times 10^{-3}$
	Tensile stress	$4.54 \times 10^{-3}$	$5.6 \times 10^{-3}$	$6.16 \times 10^{-3}$	$4 \times 10^{-3}$	$5.1 \times 10^{-3}$	$5.7 \times 10^{-3}$
	Compressive	$-4.69 \times 10^{-3}$	$-5.4 \times 10^{-3}$	$-5.6 \times 10^{-3}$	$-4.42 \times 10^{-3}$	$-5.23 \times 10^{-3}$	$-5.46 \times 10^{-3}$
Canine	von Mises	$7.6 \times 10^{-4}$	$8.2 \times 10^{-4}$	$8.6 \times 10^{-4}$	$7 \times 10^{-4}$	$7.6 \times 10^{-4}$	$8.2 \times 10^{-4}$
	Tensile	$3.58 \times 10^{-3}$	$3.69 \times 10^{-3}$	$4.3 \times 10^{-3}$	$3.1 \times 10^{-3}$	$3.4 \times 10^{-3}$	$4.2 \times 10^{-3}$
	Compressive	$-3.2 \times 10^{-3}$	$-3.4 \times 10^{-3}$	$-3.35 \times 10^{-3}$	$-3.03 \times 10^{-3}$	$-3.29 \times 10^{-3}$	$-3.26 \times 10^{-3}$
MB root of first molar	von Mises	$8.4 \times 10^{-4}$	$7 \times 10^{-4}$	$5.4 \times 10^{-4}$	$8.9 \times 10^{-4}$	$7.8 \times 10^{-4}$	$6.9 \times 10^{-4}$
	Tensile	$4.3 \times 10^{-3}$	$3.5 \times 10^{-3}$	$2.7 \times 10^{-3}$	$4.5 \times 10^{-3}$	$4.05 \times 10^{-3}$	$3.4 \times 10^{-3}$
	Compressive	$-1.4 \times 10^{-3}$	$-1.3 \times 10^{-3}$	$-1.1 \times 10^{-3}$	$-1.9 \times 10^{-3}$	$-1.8 \times 10^{-3}$	$-1.65 \times 10^{-3}$

CI, central incisor; LI, lateral incisor; MB, mesio-buccal; OMI, orthodontic mini-implants; PDL, periodontal ligament.

orthodontics, and space closure methods are always associated with some problems, of which most common is the anchorage loss. This anchorage loss, nowadays, can be prevented by the use of mini-implants. For successful en masse retraction, the forces must be in harmony with the oral tissues so that there is minimal damage to the surrounding tissues during treatment. Thus, it is very important to study the stress pattern of the periodontium to understand the effect of the forces that are being applied on the dentition during treatment. Therefore, this study was done to understand the effect of forces during en masse retraction of the anterior teeth on the periodontium with ARH and OMI at different heights.

#### 4.1. Stresses in bone

In our study, it was found that the stress values in the cortical bone were more than the cancellous bone. The probable reason for this finding might be that the cortical bone has a higher Young's modulus due to which it resists more deformation and sustains higher loads than does the cancellous bone [9]. Our results were in accordance with the study done previously [9], where the stresses in the hard bone were greater than the soft bone. All the stress values for the bone in all the models were far below the ultimate tensile strength of the bone of 135 MPa [1], indicating that the bone has sufficient strength to resist retraction forces in a clinically acceptable range.

#### 4.2. Stresses in bone surrounding implant

According to the present study, the maximum stresses were seen in the cortical bone at the mesial area of the mini-implant, which might be due to the bending of the bone in the area of the implant, which has more effect at the base support region because

of the concentration of stresses in the entrance region of the cortex than the rest of the embedded region. This result was similar to the findings of previous studies in this regard [10,11].

#### 4.3. Stresses in PDL

The PDL experiences relatively high stress on an application of orthodontic forces during tooth movement. This study showed that the concentration of the compressive stresses were at the apex on the palatal aspect of the anterior teeth. The tensile stresses were distributed at labio-cervical area of the teeth. This finding agreed with the other published studies [4,12]. The central incisors experienced fewer stresses as compared with the lateral incisors, which could be due to their PDL support, because lateral incisors have a smaller root surface area than the central incisors [13,14]. The stresses in the PDL were found to be higher at 9-mm ARH in both low and high OMI placement. Similar findings were noted in previous studies [12,15], which might be attributable to more retraction of centrals and torquing movements of laterals at 9 mm ARH.

#### 4.4. Stresses in cementum

During orthodontic movement, resorption is a common pathological phenomenon occurring at the root of the tooth. In our study, cemental stress pattern was maximum toward the mid-root and cervical area and minimum toward the apex. Under the influence of lingual tipping forces, the lingo-cervical and bucco-apical area were under compression, whereas the bucco-cervical and lingo-apical were under tension. These high-pressure zones are more susceptible to resorption, as seen in a similar study conducted previously [16]. The root apex and bony alveolar crest zone are the areas that are susceptible to greatest stress when tipping or torquing

**Table 4**  
von Mises and principal stresses in cementum (MPa)

Tooth	Stress	Low OMI (7 mm)			High OMI (10 mm)		
		3 mm	6 mm	9 mm	3 mm	6 mm	9 mm
CI	von Mises	1.09	1.06	1.02	1.13	1.08	0.99
	Tensile	0.97	0.85	0.73	1.02	0.89	0.78
	Compressive	$-2.5 \times 10^{-3}$	$-3.7 \times 10^{-3}$	$-2 \times 10^{-2}$	$-4 \times 10^{-5}$	$-5.8 \times 10^{-3}$	$-3.2 \times 10^{-2}$
LI	von Mises	2.2	3.01	3.41	2.25	2.98	3.41
	Tensile	2.09	2.3	2.68	2.02	2.04	2.6
	Compressive	$-9 \times 10^{-4}$	$-9.6 \times 10^{-3}$	$-1.13 \times 10^{-2}$	$-8.8 \times 10^{-4}$	$-1.04 \times 10^{-2}$	$-1.2 \times 10^{-2}$
Canine	von Mises	11.3	10.7	9.51	10.14	9.7	8.6
	Tensile	2.4	2.9	3.2	2.3	2.9	3.2
	Compressive	-1.982	-1.981	-1.6	-1.8	-1.6	-1.39
MB root of first molar	von Mises	3.75	3.714	3.42	3.1	3.04	2.7
	Tensile	1.6	2.09	2.26	0.8	0.9	1.14
	Compressive	-1.06	-1.029	-0.9	-0.7	-0.81	-0.79

CI, central incisor; LI, lateral incisor; MB, mesio-buccal; OMI, orthodontic mini-implants.

**Table 5**  
Displacement along y- and z-axis (mm)

Tooth	Reference point	Low OMI (7 mm)			High OMI (10 mm)		
		Hook height (mm)	Δy (mm)	Δz (mm)	Hook height (mm)	Δy (mm)	Δz (mm)
CI	RA	3 mm	6.5E-03	-2.4E-03	3 mm	6.1E-03	-1.6E-03
	IE		8.65E-03	-4.01E-03		8.3E-03	-3.1E-03
	RA	6 mm	7.2E-03	-3.7E-03	6 mm	7.04E-03	-3E-03
	IE		9.2E-03	-5.2E-03		9.02E-03	-4.4E-03
	RA	9 mm	7.3E-03	-4.5E-03	9 mm	7.17E-03	-3.8E-03
	IE		9.04E-03	-5.7E-03		8.9E-03	-5.1E-03
LI	RA	3 mm	7.6E-03	-3.08E-03	3 mm	7.4E-03	-2.2E-03
	IE		8.7E-03	-3.33E-03		7.9E-03	-2.4E-03
	RA	6 mm	8.65E-03	-4.51E-03	6 mm	8.5E-03	-3.9E-03
	IE		9.12E-03	-4.4E-03		8.8E-03	-3.7E-03
	RA	9 mm	9.26E-03	-5.5E-03	9 mm	9.1E-03	-4.91E-03
	IE		8.96E-03	-4.9E-03		8.6E-03	-4.4E-03
Canine	RA	3 mm	3.51E-03	-1.98E-03	3 mm	3.7E-03	-1.3E-03
	IE		9.09E-03	-4.16E-03		8.8E-03	-3.2E-03
	RA	6 mm	2.77E-03	-2.47E-03	6 mm	3.7E-03	-1.8E-03
	IE		9.41E-03	-5.89E-03		9.2E-03	-5.1E-03
	RA	9 mm	1.97E-03	-2.66E-03	9 mm	2.2E-03	-2.1E-03
	IE		9.16E-03	-6.82E-03		9.03E-03	-7.3E-03
MB root of first molar	RA	3 mm	-0.6E-03	-0.11E-03	3 mm	-6E-05	-5.8E-04
	IE		0.4E-03	-0.29E-03		1.5E-03	-8.2E-04
	RA	6 mm	-0.41E-03	-0.27E-03	6 mm	1.2E-04	-2.5E-04
	IE		0.21E-03	-0.22E-03		1.3E-04	-2.5E-04
	RA	9 mm	-0.23E-03	-0.61E-03	9 mm	2.4E-04	-1.8E-04
	IE		0.08E-03	-0.6E-03		8.5E-04	-8E-05

CI, central incisor; LI, lateral incisor; MB, mesio-buccal; OMI, orthodontic mini-implants.

movements are seen [17]. A possible reason could be that when the forces are applied, the stress is dissipated in the alveolar crest and mid-root area before it reaches to apex. Hence, significant stress is not seen in the apical region. The compressive stresses were more on the lateral incisors than the centrals. It may be because of their smaller root surface area as compared with central incisors as, stated in a study by Hemanth et al. [18].

4.5. Displacement along the y- and z-axis

In all the models, extrusion was seen along with the lingual tipping of the incisors and distal tipping of the canines under the influence of retractive forces acting on the anterior segment. In our study, at the 3-mm and 6-mm ARH, lingual tipping of anterior teeth was noticed compared with torquing movements seen at 9-mm ARH. Similar findings were seen in the literature [4], where high OMI traction with high ARH lead to controlled tipping of the centrals and in laterals, the root apex moved more lingually, whereas at 3-mm and 6-mm ARH, tipping movements were noticed. The reason for the overall tipping in the models at 3-mm and 6-mm ARH is that the line of action of force was below the CR of the anterior segment. At 9-mm ARH, the force vector was very near to the estimated CR at 7-mm implant placement and above the CR at 10-mm implant placement. So, it can be concluded that the CR plays a crucial role on the type of the tooth movement in orthodontics.

In our study, the CR was assumed according to the findings in a previous study [19], which was 13.5 mm posterior and 9 mm apical from the center of the archwire. In true sense, we should identify the CR for the 6 anterior teeth in the base model to apply the force closer to it in order to achieve the desired results. The CR varies among patients, depending on various factors, such as root length, bone support, and number of teeth, as stated in previous studies [20–23]. The model in our finite element study was fabricated from the CT scan of a patient. Because the CR varies among patients, the CR of our patient also could have differed in the anatomical location from the actual CR.

In the z-axis, the extrusion was seen in all the models. The extrusion increased with the increase in the height of the retraction hook. Similar findings were reported in another studies [4,6]. In

another study, the author observed that, the shorter the ARH height, the better the crown torque was maintained and hence recommended short ARH [24]. In our study, the models with low ARH height of 3 mm showed the least amount of extrusion with maximum at high ARH (9 mm). This might be because of the change in  $\theta$  angle, which can alter the paradigm of biomechanics. Increasing the height of the anterior power arm would cause a decrease in the  $\theta$  angle but would increase the horizontal force (horizontal force = force  $\times$   $\cos\theta$ ) and decreasing the  $\theta$  angle can reduce the vertical force (vertical force = force  $\times$   $\sin\theta$ ) as quoted in a study [25]. The amount of lingual tipping and extrusion was less in the high OMI group compared with low OMI group. According to another study [25], for every millimeter of implant placed apically, the  $\theta$  angle increases by 2°, hence, reducing the retraction component of force by 1% and increasing the intrusion component of force by approximately 0.3%.

The retraction force with mini-screw anchorage also produced rotation of the entire arch around the CR near the premolar root, which resulted in extrusion of anterior teeth, maximum in canines and least in molars. Similar findings were reported in the literature [26]. The bracket can also play a crucial role during retraction. In the present study, we used 0.019  $\times$  0.025-inch SS wire in 0.022  $\times$  0.028-inch slot system. Because there was play present in the wire bracket interface, deformation of the wire must have taken place, which might be the most probable reason for the clockwise rotation of the occlusal plane. Similar results were noted in the literature [27].

**Table 6**  
Change in inclination for anterior teeth (degrees)

Tipping angle for anterior teeth			
	Central incisor	Lateral incisor	Canine
Implant at 7 mm			
3 mm Power Arm	0.8	0.5	1.5
6 mm Power Arm	1.1	0.7	1.9
9 mm Power Arm 1.3	1.3	0.9	1.7
Implant at 10 mm			
3 mm Power Arm	0.6	0.4	1.2
6 mm Power Arm	0.9	0.6	1.4
9 mm Power Arm	1.1	0.8	1.3

#### 4.6. Limitations of the study

The results of our study are valid only for the initial tooth movement produced by elastic deformation of the PDL. The long-term orthodontic movement varies with the force system and therefore cannot be predicted. Moreover, in this study, PDL was considered to be a linear structure, whereas in actual terms it is a nonlinear structure [28]. Thus, actual stresses could have been analyzed if the PDL was considered as a nonhomogeneous structure. Also, CR was not calculated for the present study and it was assumed according to the previous literature, which also should have been taken into consideration. The simulation in the FEM study is based on mechanical laws, and this method may not be sufficient for predicting orthodontic tooth movement in the clinical scenario. Therefore, FEM results should be correlated with preclinical and long-term clinical studies to validate research models [29].

#### 4.7. Clinical implications of the study

In Class II Division 1 patients, controlled retraction of maxillary anteriors can be obtained with the combination of high OMI and ARH of 3 to 6 mm. In Class II Division 2 cases, the palatal root torque of the incisors can be achieved by increasing the height of ARH to 9 mm.

### 5. Conclusions

The following conclusions can be drawn from the present study:

1. An overall tipping and extrusion was seen in all the models. The tipping was more in low OMI models as compared with the high OMI models.
2. The lingual tipping of the anterior teeth was more at 3-mm and 6-mm ARH, whereas at 9-mm ARH, more of bodily movement with lingual root movement was seen in both high and low OMI models.
3. An overall clockwise rotation of the occlusal plane was noticed with the extrusion of the anteriors and slight extrusion of the posteriors.
4. The laterals had more stresses in PDL and cementum compared with centrals in all the models.
5. The distribution of stresses was in the apical and alveolar crest area, making these areas more prone to resorption.

### References

- [1] Creekmore TD, Eklund MK. The possibility of skeletal anchorage. *J Clin Orthod* 1983;17:266–9.
- [2] Martins DR, Tibola D, Janson G, Maria FRT. Effects of intrusion combined with anterior retraction on apical root resorption. *Eur J Orthod* 2012;34:170–5.
- [3] Cattaneo PM, Dalstra M, Melsen B. The finite element method: a tool to study orthodontic tooth movement. *J Dent Res* 2005;84:428–33.
- [4] Sung SJ, Jang GW, Chun YS, Moon YS. Effective en-masse retraction design with orthodontic miniimplant anchorage: a finite element analysis. *Am J Orthod Dentofacial Orthop* 2010;137:648–57.
- [5] Uzuka S, Chae J-M, Tai K, Tsuchimochi T, Park JH. Adult gummy smile correction with temporary skeletal anchorage devices. *Journal of the World Federation of Orthodontists* 2018;7(1):34–46.
- [6] Bohara P, Kumar M, Sharma H, Jayprakash P, Misra V, Savana K. Stress distribution and displacement of maxillary anterior teeth during en-masse intrusion and retraction: a FEM study. *J Indian Orthod Soc* 2017;51:152.
- [7] Parashar A, Reddy K, Reddy M, Shashidar NR, Mallikarjun V, Parik N. Torque loss in en-masse retraction of maxillary anterior teeth using miniimplants with force vectors at different levels: 3D FEM study. *J Clin Dia Res* 2014;8:ZC77–80.
- [8] Machado GL. Effect of orthodontic mini screw placement angle and structure on stress distribution at bone miniscrew placement—3D FEA. *Saudi J Dent Res* 2014;5:73–80.
- [9] Namburi M, Nagothu S, Kumar C, Chakrapani N, Hanumantharao C, Kumar S. Evaluating the effects of consolidation on intrusion and retraction using temporary anchorage devices—a FEM study. *Prog Orthod* 2017;18:2.
- [10] Liu TC, Chang CH, Wong TY, Liu JK. Finite element analysis of miniscrew implants used for orthodontic anchorage. *Am J Orthod Dentofacial Orthop* 2012;141:468–76.
- [11] Mohammed MA, Mohamed KM. Three-dimensional stress analysis with two molar protraction techniques using Finite Element Modeling. *Journal of the World Federation of Orthodontists* 2018;7(3):89–93.
- [12] Zhang DQ, Su JH, Xu LY, Zhong PP. 3-D finite element analysis on centre of resistance of upper anterior teeth. *Shanghai Kou Qiang Yi Xue* 2010;19:534–40.
- [13] Phillips JR. Apical root resorption under orthodontic therapy. *Angle Orthod* 1955;25:1–22.
- [14] Ketcham AH. Factors affecting root resorption. *Int J Orthod Oral Surg* 1929;25:310–28.
- [15] Park HS, Kwon TG. Sliding mechanics with microscrew implant anchorage. *Angle Orthod* 2004;74:703–10.
- [16] Oppenheim A. Human tissue response to orthodontic intervention of short and long duration. *Am J Orthod Oral Surg* 1942;28:263.
- [17] Puente MI, Galban L, Cobo JM. Initial stress differences between tipping and torque movements—a three-dimensional finite element analysis. *Eur J Orthod* 1996;18:329–39.
- [18] Hemanth M, Deoli S, Raghuvver HP, Rani MS, Hegde C, Vedavathi B. Stress induced in the periodontal ligament under orthodontic loading (part I): a finite element method study using linear analysis. *J Int Oral Health* 2015;7:129–33.
- [19] Melsen B, Fotis V, Burstone CJ. Vertical force considerations in differential space closure. *J Clin Orthod* 1990;24:678–83.
- [20] Dermaut LR, Vanden Bulcke MM. Evaluation of intrusive mechanics of the type "segmented arch" on a macerated human skull using the laser reflection technique and holographic interferometry. *Am J Orthod* 1984;89:251–63.
- [21] Pedersen E, Isidor F, Gjessing P, Andersen K. Location of centres of resistance for maxillary anterior teeth measured on human autopsy material. *Eur J Orthod* 1991;13:452–8.
- [22] Shroff B, Lindauer SJ, Burstone CJ, Leiss JB. Segmented approach to simultaneous intrusion and space closure: biomechanics of the three-piece base arch appliance. *Am J Orthod Dentofacial Orthop* 1995;107:136–43.
- [23] Reimann S, Keilig L, Jager A, Bourauel C. Biomechanical finite element investigation of the position of the centre of resistance of the upper incisors. *Eur J Orthod* 2007;29:219–24.
- [24] Song WJ, Lim KJ, Lee JK, Sung JS, Chune YS, Mo SS. Finite element analysis of maxillary incisor displacement during en-masse retraction according to orthodontic mini-implant position. *Korean J Orthod* 2016;46:242–52.
- [25] Chetan S, Keluskar KM, Vasisht VN, Revankar S. En-masse retraction of the maxillary anterior teeth by applying force from four different levels—a finite element study. *J Clin Diagn Res* 2014;8(9):ZC26.
- [26] Jung MH, Kim TW. Biomechanical considerations in treatment with miniscrew anchorage. Part 1: the sagittal plane. *J Clin Orthod* 2008;42:79–83.
- [27] Tominaga JY, Chiang PC, Hiroya O, Tanaka M, Koga Y. Effects of bracket slot and archwire on anterior tooth movement during space closure in sliding mechanics. *Am J Orthod Dentofacial Orthop* 2014;146:166–74.
- [28] Uhlir R, Mayo V, Hua P, Chen S, Lee Y, Hershey G. Biomechanical characterization of the periodontal ligament: orthodontic tooth movement. *Angle Orthod* 2017;87:183–92.
- [29] Kojima Y, Kawamura J, Fukui H. Finite element analysis of the effect of force directions on tooth movement in extraction space closure with miniscrew sliding mechanics. *Am J Orthod Dentofacial Orthop* 2012;142:501–8.